Available online at www.sciencedirect.com
SCIENCE DIRECT
Journal of Catalysis 229 (2005) 283–297
JOURNAL OF CATALYSIS
www.elsevier.com/locate/jcat

Novel Pt^0 catalysts supported on functional resins for the chemoselective hydrogenation of citral to the α,β-unsaturated alcohols geraniol and nerol

P. Centomo [a], M. Zecca [a,*], S. Lora [b], G. Vitulli [c], A.M. Caporusso [d], M.L. Tropeano [e], C. Milone [e], S. Galvagno [e,*], B. Corain [a,f,*]

[a] *Dipartimento di Scienze Chimiche, Via Marzolo 1, 35131 Padova, Italy*
[b] *Istituto per la Sintesi Organica e la Fotoreattività, C.N.R., via Romea 4, 35020 Legnaro, Italy*
[c] *Istituto di Chimica dei Composti Organometallici, c/o Dipartimento di Chimica e di Chimica Industriale Via Risorgimento 35, 56126 Pisa, Italy*
[d] *Dipartimento di Chimica e di Chimica Industriale Via Risorgimento 35, 56126 Pisa, Italy*
[e] *Dipartimento di Chimica Industriale, Salita Sperone 31, 98166 Messina, Italy*
[f] *Istituto di Scienze e Tecnologie Molecolari, C.N.R., Sezione di Padova c/o Dipartimento di Scienze Chimiche, Via Marzolo 1, 35131 Padova, Italy*

Received 23 July 2004; revised 5 October 2004; accepted 6 October 2004

Available online 23 December 2004

Abstract

Nanoclustered Pt^0 catalysts based on cross-linked macromolecular matrices are evaluated in the hydrogenation of an α,β-unsaturated aldehyde (citral). Matrices and catalysts are characterized by inverse steric exclusion chromatography, scanning electron microscopy, X-ray microprobe analysis, and transmission electron microscopy. The monometallic catalysts exhibit remarkable selectivity for geraniol/nerol when 2–3-nm, regularly shaped, spherical metal nanoclusters are deposited on the supports from solutions of solvated platinum atoms prepared by metal vapor synthesis (MVS). The immobilization in the polymer framework of ions of a second metal such as Fe(II), Co(II), or Zn(II) enhances the selectivity of the Pt catalysts by up to more than 90%.

Keywords: Nanoclustered platinum(0); Functional resins; Selective hydrogenation; α,β-Unsaturated aldehyde

1. Introduction

The selective hydrogenation of α,β-unsaturated aldehydes to α,β-unsaturated alcohols is a frequently occurring step in the industrial synthesis of specialty chemicals, typically in the liquid phase [1]. The reaction is known to be effectively catalyzed by group VIII metal complexes in the liquid phase [2] and by supported group VIII metal nanoclusters under both solid–gas [3] and liquid–solid conditions [4]. The selectivity for α,β-unsaturated alcohols in liquid–solid heterogeneous catalysis has been found to depend critically on a variety of parameters, such as the nature of the active noble metal [1,5], the nature of the support [3,6], and the metal nanocluster size [1]. Improved selectivity can be obtained with bimetallic catalysts, where the second metal (Sn, Ge, Co, etc.) is more electropositive than the noble one [3,7]. The electropositive metal is supposed to release electronic density to the noble metal. On one hand, this makes the active metal more electron rich and therefore disfavors the adsorption of the unsaturated aldehyde through the double C–C bonds and the hydrogenation thereof. On the other hand, the electropositive metal becomes electron-deficient and forms sites where carbonyl groups stick through their nucleophilic oxygen atoms. This favors the hydrogenation of the double C–O bonds. An improved selectivity for unsaturated alcohols is also observed when bases (of both the Brønsted or Lewis type) are dissolved in the reaction mixture. These electron-donating species are supposed to interact with the metal surface, thus increasing its electron density [1]. This is not the only way in which the catalytic process can be modified; for steric reasons the basic species lying on the

* Corresponding authors. Fax: 049-8275223; 049-8275223.
E-mail address: benedetto.corain@unipd.it (B. Corain).

0021-9517/$ – see front matter
doi:10.1016/j.jcat.2004.10.018

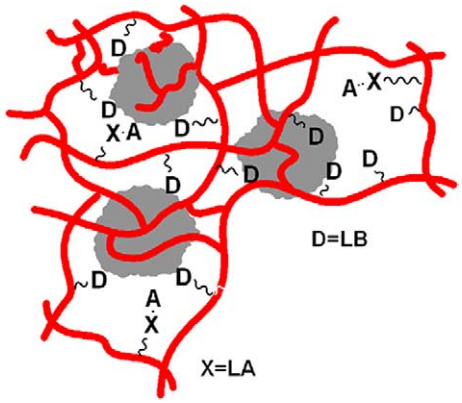

Fig. 1. The concept of a "multitasking" catalyst supported by a functional resin. A: Lewis acid units (typically a metal ion); X: metal coordinating or ion-exchanging functions; D: Lewis base units.

metal surface likely favors "end-on" adsorption of the unsaturated aldehyde molecules, which is possible only if they approach the metal surface with the carbonyl group. This circumstance further reduces the catalyst's capacity to hydrogenate double C–C bonds. Finally, several Lewis acids added to the reaction mixture are able to enhance the selectivity with α,β-unsaturated alcohols [1,8]. In this case, they are supposed to interact with the oxygen atoms of the carbonyl groups. As a result, the C–O bond is polarized and the carbonyl carbon atom becomes more susceptible to the nucleophilic attack of the hydridic adsorbed hydrogen atoms [1].

The use of soluble basic and acidic promoters at the same time is clearly not feasible under classic conditions; the base and the acid would neutralize each other. This could be possible if basic and acidic promoters were conveyed to the "microenvironment" of the metal nanoclusters inside of a heterogeneous catalyst in such a way as to prevent their direct interaction. Multiple promotion effects would take place cooperatively in a catalyst of this kind ("multitasking" catalyst). Designed polyfunctional resins (Fig. 1) possessing both basic and acidic functions chemically connected to the polymeric chains are potentially able to do this.

We report here on the catalytic behavior of various resin-supported platinum catalysts in the hydrogenation of citral in ethanol at 333 K and 105 kPa. Currently citral is one of the most intensively investigated substrates [9], along with crotonaldehyde [10] and cynnamic aldehyde [11], for the selective hydrogenation of the carbonyl group. In comparison with the latter two, citral has an even more complex regiochemistry, in that it possesses three double bonds; the most difficult to reduce is the carbonyl bond (Scheme 1).

The resins employed herein as supports contain different functional groups, most of which are basic in nature. They are either used as such or after the introduction of metal ions (Lewis acids). The use of polymeric supports for the heterogeneous solid–liquid hydrogenation of α,β-unsaturated aldehydes is not unprecedented. A previous example of active and very selective Pt/polystyrene catalyst

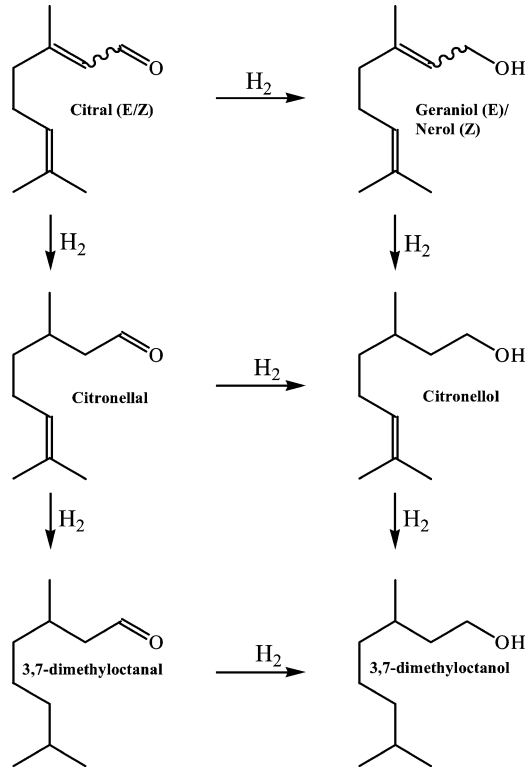

Scheme 1.

for the transformation of cynnamic aldehyde to cinnamyl alcohol in ethanol at 333 K and 4.0 MPa is reported in Ref. [12].

2. Experimental

2.1. Materials and apparatus

X-ray microprobe analysis was carried out with a Cambridge Stereoscan 250 EDX PW 9800. Transmission electron microphotographs (TEMs) were taken with either a JEOL 2010 microscope with GIF operated at an accelerating voltage of 200 keV or a Philips CM200 microscope (ultrafine sections). A home-assembled apparatus made available by Dr. K. Jerabek (Institute of Chemical Process Fundamentals, Czech Academy of Sciences, Prague–Suchdol) was used for inverse steric exclusion chromatography. Experimental details of the basic operation and choice of the probes are given in Ref. [19]. The amount of platinum in the MVS-derived solutions was determined, after mineralization, by atomic absorption spectrometry in a electrothermally heated graphite furnace with a Perkin-Elmer 4100 ZL instrument with longitudinal Zeeman effect background corrector. Chemical analyses of the hydrogenation mixtures were performed with a Shimadzu GC17A gas chromatograph, equipped with an EC-WAX wide-bore capillary column (60 m, 0.53 mm i.d.). Monomers for the synthesis of the resins, analytical-grade metal acetates, $NaBH_4$, and ethanol for the preparation of CIR catalysts were supplied by

Aldrich. $[Pt(NH_3)_4]Cl_2$ was prepared according to methods described in the literature [13], starting from $PtCl_2$ (Aldrich) and aqueous concentrated ammonia (C. Erba). Mesitylene and *n*-pentane were purified by conventional methods, distilled, and stored under argon. Analytical-grade citral and ethanol, used in the catalytic tests, were supplied by Aldrich and Fluka, respectively. If not otherwise stated, chemicals from commercial sources were used as received from the supplier.

2.2. Sample preparation for TEM

Some samples were obtained by mechanical milling of the as-prepared solid sample and subsequent dispersing in ethanol with an ultrasonic bath for 0.5 h. One drop of the suspension obtained in this way was placed on a carbon-coated copper grid, dried at room temperature, and then put into the microscope. Some samples were obtained by embedding the material in Araldite CY212 and, after polymerization, by cutting 30-nm slices with a Leica Ultracut-R ultramicrotome.

2.3. Resin synthesis

The procedure for synthesizing functional resins has been carefully described in Ref. [14]. The only difference in our method was in the thorough washing of the crude and ground resins (sieved to 180–400 μm) with methanol in a Soxhlet apparatus for 4 days. CF4 resin is commercially available from Aldrich (poly-4-vinylpyridine-divinylbenzene, 2% mol).

2.4. Metalation of CF3{70} with $[Pt(NH_3)_4]Cl_2$

The functional resin (ca. 1 g) is suspended in water and left under moderate stirring for 2 h. About 0.3 g of $NaBH_4$, dissolved in 10 ml of water, is added under manual stirring and left under moderate magnetic stirring until the gas release stops. Sodium-form resin is filtered and washed with water. The sample is suspended in water (ca. 50 ml) and left under moderate stirring for 2 h. About 26 mg (0.94 mmol) of $[Pt(NH_3)_4]Cl_2$ dissolved in 5 ml of water is added under manual stirring and left under moderate mechanical stirring for about 1 day. The resin color does not change appreciably. One milliliter of surnatant phase (ca. 1/60 of the total amount of the liquid phase) is treated with 5 mg $NaBH_4$. The absence of any precipitated platinum black indicates practically quantitative incorporation of Pt^{II} (in the case where there is no incorporation of platinum, it would have been reduced by only 0.6 mg $NaBH_4$). Metalated resins are filtered, washed with water, and dried in vacuo at 60 °C.

2.5. Reduction with $NaBH_4$ in water

The metalated resin (ca. 1 g, ca. 1% mol Pt) is suspended in ca. 10 ml water and left under moderate stirring for 2 h.

Table 1
Metalation of CF3 with $M(OAc)_2$ ($M = Fe^{II}$, Zn^{II}, Co^{II})

Metal precursor	Precursor weight (g)	CF3 weight (g)
$Fe(OAc)_2$	1.12	1.01
$Zn(OAc)_2$	1.51	1.00
$Co(OAc)_2$	1.43	1.02

About 300 mg (7.9 mmol) of $NaBH_4$ dissolved in 10 ml water are added under manual stirring with consequent vigorous gas evolution and left under moderate mechanical stirring for ca. 90 min, after which the liquid phase appears to be colorless and the resins have become black. The reduced sample is filtered, washed with water and methanol, and dried in vacuo at 60 °C to constant weight. A black powder is obtained.

2.6. Metalation of CF3 with $M(OAc)_2$ ($M = Fe^{II}$, Zn^{II}, Co^{II})

Functional resin (ca. 1 g) is suspended in water and left under moderate stirring for 2 h. The metal precursor (Table 1) dissolved in ca. 20 ml of water is added. The solvent and the acetic acid produced during the metalation reaction are removed with the use of a rotating evaporator (ca. 50 °C, 6 mm Hg) until incipient wetness. A further 50 ml of water is added. The evaporation procedure is repeated five times. If the metal precursor is colored (Fe^{II} and Co^{II}) it is possible to follow the reaction progress from the fading of solution color, and the concomitant coloration of the resin particles. The sample is filtered, washed with water and methanol, and dried in vacuo at 60 °C to constant weight.

2.7. Metalation of CF4 with $Co(OAc)_2$

CF4 (0.2 g, 1.8 mmol of pyridyl groups) is suspended in ca. 5 ml of ethanol. After overnight standing, 0.226 g of $Co(OAc)_2 \cdot 4H_2O$ (0.9 mmol of cobalt) dissolved in the minimum amount of ethanol is added to the alcoholic suspension of the resin. After 5 h of moderate stirring at room temperature, the suspension is filtered. The recovered solid is washed three times with 10 ml of fresh ethanol and finally dried to constant weight.

2.8. MVS synthesis

In a typical experiment, Pt-vapor, generated by resistive heating of a W wire surface coated with electrodeposited Pt (100–200 mg), is co-condensed at a liquid nitrogen temperature with mesitylene (70 ml) in a glass reactor described elsewhere [15]. The reactor chamber is warmed at the melting point of the solid matrix (−30 °C), and the resulting yellow–brown solution is siphoned and handled at low temperature (−30/−40 °C) with the Schlenk tube technique. The content of the metal is 1 mg/ml. To a suspension of the desired functional resin (2 g) in mesitylene (5 ml) is added the required amount of the above Pt/mesitylene solution to

obtain the supported final platinum catalyst. The mixture is stirred for 24 h at room temperature. The colorless solution is removed and the brown material is washed three times with previously deareated *n*-pentane and dried at room temperature under reduced pressure (10^{-2} Torr).

2.9. Catalytic tests

Catalytic experiments are carried out at atmospheric pressure under H_2 flow, at 60 °C, in a four-necked flask fitted with a reflux condenser, dropping funnel, thermocouple, and a stirrer head. The catalyst is added to 25 ml of solvent and reduced in situ at 70 °C for 1 h. After cooling at reaction temperature, the substrate (0.5 ml) is injected through one arm of the flask. The reaction mixture is stirred at 700 rpm. The progress of the reaction was followed by gas chromatographic analysis of a sufficient number of microsamples. Selectivities are calculated from the expression $S_i = C_i \cdot [\sum C_p]^{-1}$, where C_i is the concentration of the ith product and C_p is the total concentration of the products.

3. Results and discussion

3.1. Synthesis of functional resins

We have synthesized two sets of functional gel-type resins. One consists of CF1, CF2, and CF3 (Scheme 2), which contain only one functional monomer (respectively: *N*,*N*-dimethyl-2-aminoethylmethacrylate, DMAEMA; cyanoethyl-acrylate, CEA; methacrylic acid, MA) and the cross-linker (divinylbenzene, DVB). The other comprises CF2{50}, CF3{30}, CF3{50}, and CF3{70} (Scheme 3), which contain the functional monomer (CEA for the first, MA for the others), *N*,*N*-dimethylacrylamide (DMAA), and the cross-linker (divinylbenzene, DVB). CF4 (a homopolymer of 4-vinylpyridine) is a commercial resin, 2% cross-linked with DVB, commercially available as irregular submillimetric particles. The resins employed here are generally gel-type, that is, they do not possess a macropore system in the dry state. Microporosity develops only when they are swollen with suitable liquid agents. CF4 is somewhat different from the other materials, and its morphology was investigated separately [16].

The design of resins CF1, CF2, and CF3 and the choice of CF4 rest on the idea of employing polymer frameworks featured by either Lewis basic groups or by a functional group (–COOH in the case of CF3) able to bind metal centers and possibly able to promote the metal catalysts.

Resins CF2-50, CF3{30}, CF3{50}, and CF3{70} are also gel-type resins. They are copolymers of *N*,*N*-dimethylacrylamide (DMAA) and CEA (CF2-50) or MA (CF3{30}, CF3{50}, CF3{70}). The respective molar fractions of DMAA (30, 50, 70%) are indicated by the relevant codes.

All resins are obtained in very high yields upon γ-irradiation at room temperature [17]. After work-up of the crude materials (see Section 2), they are eventually obtained as 180–400-μm particles. Synthetic and analytical details are collected in Tables 2–5.

As discussed below, a marked swelling ability of the polymeric supports in ethanol is a desirable feature. In par-

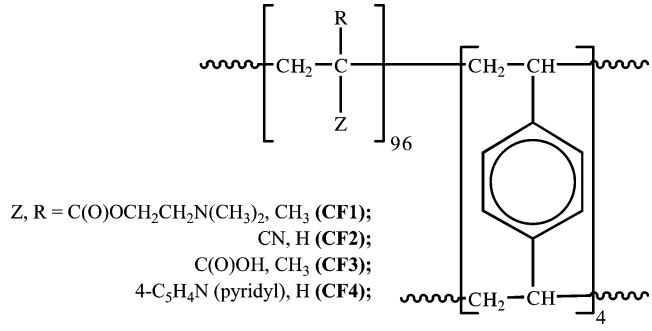

Scheme 2.

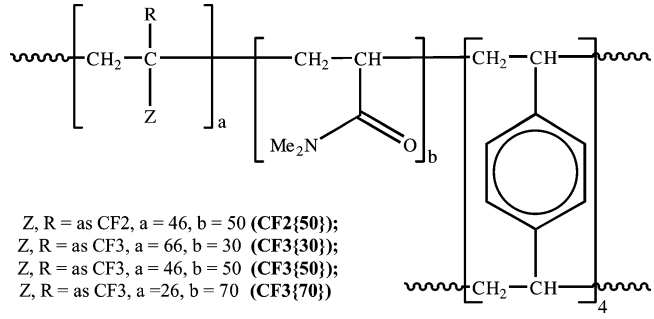

Scheme 3.

Table 2
Synthetic details for resins CF1, CF2, and CF3

	DMEDMA	AMA (mmol)	CEA (mmol)	DVB (mmol)	Yield (%)
CF1	200	–	–	9	91
CF2		–	240.8	18.8	94
CF3		355.8	–	26.8	93

Table 3
Analytical data on resins CF1, CF2, and CF3

	Found			Expected[a]		
	C (%)	H (%)	N (%)	C (%)	H (%)	N (%)
CF1	62.60	9.46	8.18	65.52	10.17	7.40
CF2	59.40	5.70	10.42	59.11	5.69	10.72
CF3	57.60	6.91	–	57.63	6.92	–

[a] For 100% polymerization yield.

Table 4
Synthetic details of resins CF2-50, CF3{30}, CF3{50}, and CF3{70}

	AMA (mmol)	CEA (mmol)	DMAA (mmol)	DVB (mmol)	Yield (%)
CF2-50	–	16.9	44.4	3.8	94
CF3{30}	71.6	–	32.5	4.7	95
CF3{50}	48.9	–	52.5	4.6	95
CF3{70}	26.7	–	72.7	4.3	94

Table 5
Analytical data on resins CF2-50, CF3{30}, CF3{50}, and CF3{70}

	Found			Expected[a]		
	C (%)	H (%)	N (%)	C (%)	H (%)	N (%)
CF2-50	60.64	6.98	11.47	63.64	7.92	11.57
CF3{30}	58.78	7.42	3.90	61.17	7.70	4.34
CF3{50}	54.94	7.89	6.07	62.02	8.10	6.99
CF3{70}	53.42	7.95	8.74	62.58	8.49	9.70

[a] For 100% polymerization yield.

ticular, one of the ways of preparing the catalysts used in the current study implies the dispersion of the active metal (platinum) throughout the whole volume of the catalyst particles [17]. A high degree of swelling in the reaction solvent is therefore required to ensure a good accessibility of platinum. It is convenient to anticipate here that in the case of the MA-based materials, this protocol implies the transformation of the carboxylic resins into their sodium forms, which also should be able to swell in ethanol. The introduction in the polymer framework of DMAA as a comonomer along with either CEA (CF2{50}) or MA (CF3{30}, CF3{50}, CF3{70}) is a response to the necessity for materials that undergo marked swelling in ethanol. Our previous experience has shown that DMAA is suited to this purpose, while keeping an amphiphilic character [18]. As discussed below, this prediction has been confirmed for CF2-50 and CF3{70} (Table 6) by BEV (bulk expanded volume) values [18] in ethanol and, at least as a trend, by inverse steric exclusion chromatography (ISEC) analysis in water [19].

3.2. SEM characterization

Resin morphology is evaluated with scanning electron microscopic (SEM) analysis, which confirms the expected [20] gel-type character of CF1, CF2, and CF3, though very few particles of CF3 exhibit a sort of macroporosity (Fig. 2e). Fig. 2 illustrates at convenient magnification the typical glassy aspect of gel-type resins in the dry state. CF4 exhibits a complex micro- and nanomorphology whose details will be given elsewhere [16]. It exhibits micrometer-wide "channels" that favor overall accessibility of the polymeric mass, and it is akin to macroreticular resins in this respect. However, we have collected evidence that local swelling occurs in a relatively thin layer of polymer mass just beneath the surface of the aforementioned "channels." Therefore, chemistry within CF4 can take place not only *on* the pore walls, but also *in* the swollen layer of polymeric gel.

3.3. BEV and SAV characterization

The capacity of the investigated resins to swell was evaluated from BEV [18] and specific absorbed volume (SAV) [21] at a semiquantitative level, and with ISEC (see below) at a quantitative level. BEV is defined as $(V_g - V_0)g^{-1}$, where V_g is the final specific swollen volume and V_0 is the initial volume of dry, carefully sieved and properly packed resins (180–400 μm). SAV is defined as milliliters of absorbed solvent per gram of resin. BEV measurements were carried out in water, ethanol, and mesitylene, the most important solvents used in this investigation. In particular, water and mesitylene are used in the metalation reactions and ethanol in the hydrogenation tests.

Table 6
BEV of CF1, CF2, CF3, CF3/Na^+ in water and ethanol

Support	BEV (ml/g)		
	Water	Ethanol	Mesitylene
CF1	1.6	1.7	–
CF2	0.5	0.4	0.0
CF2-50	1.3	1.2	–
CF3	1.8	2.0	0.3
CF3{30}	0.6	1.1	–
CF3{50}	1.2	1.2	–
CF3{70}	3.0	2.2	–
CF3/Na^+	5.0	0.0	–
CF3{30}/Na^+	–	0.2	–
CF3{50}/Na^+	–	0.0	–
CF3{70}/Na^+	–	1.8	–

The data of Table 6 show that CF2 swells to a very little extent. However, when DMAA is introduced in the polymer backbone (50% mol), the degree of swelling increases strongly in both solvents. In fact, this comonomer makes the resin more compatible with polar solvents like water and ethanol [22]. This is also confirmed by ISEC analysis (see next section). CF3 swells rather well in both water and ethanol. In this case, partial dissociation of the (weakly acidic) carboxylic groups creates fixed negative charges, and the repulsive forces among them enhance the degree of swelling. In ethanol, the degree of swelling of the polymer is slightly higher. Dilution of the carboxylic groups with DMAA reduces this electrostatic contribution, and therefore CF3{30} and CF3{50} swell less than CF3. However, at a high DMAA molar fraction the affinity for polar solvents due to the presence of this comonomer prevails and CF3{70} swells more than CF3. When the H^+ ion is replaced by a Na^+ ion (CF3/Na^+), the polymer swells much better in water, but not at all in ethanol. For CF3/Na^+ the Doonan effect is strongly enhanced in water, because all of the carboxylic groups are present as ionic pairs (–COO^-/Na^+) that are completely separated because of effective solvation of the Na^+ ions. In ethanol, solvation of the Na^+ ions is not as strong, and the contribution of the electrostatic repulsion to swelling is apparently lost. Again, the introduction of substantial amounts of DMAA in the MA-based resins makes them more compatible with ethanol, but as much as 70% (molar) DMAA is needed to achieve an acceptable degree of swelling of the sodium form of the support in ethanol.

3.4. ISEC characterization

The effect on swelling of the gradual introduction of DMAA in the CEA- and MA-based resins in water was as-

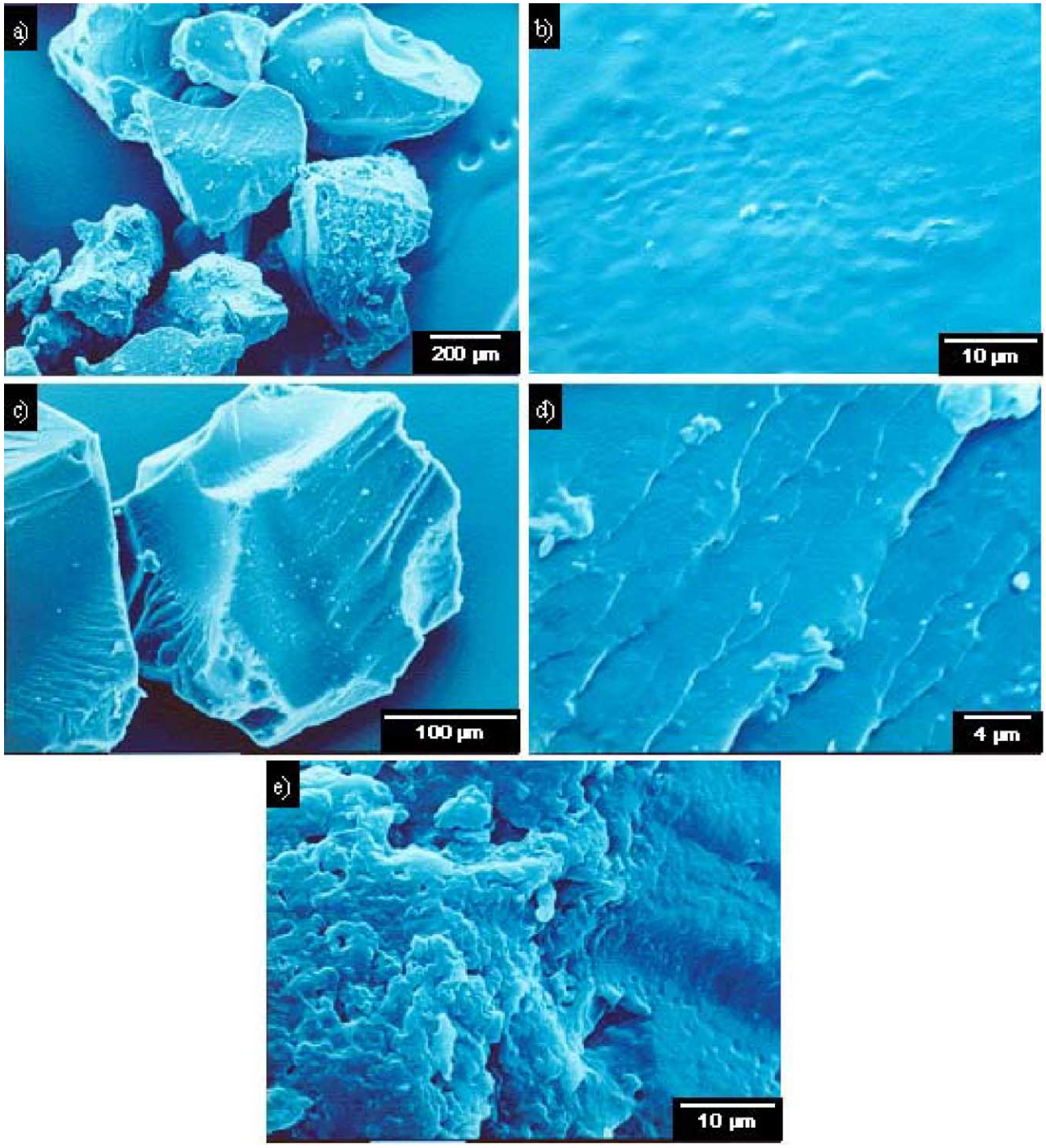

Fig. 2. SEM picture of resin CF2 ((a) 150×; (b) 2500×) and CF3 ((c) 350×; (d) 2500×; (e) 5000×).

sessed by means of ISEC analysis. When functional resins are put in contact with suitable liquids, swelling of the polymer matrix occurs, and its swollen-state morphology becomes substantially different from the dry-state morphology. Therefore, information based on conventional porosimetric techniques, like nitrogen adsorption or mercury penetration, is not useful in this respect. A quantitative description of the swollen-state morphology of polymer materials can be obtained with ISEC. This method is based on measurements of elution volumes of a number of standard solutes of known molecular sizes, flowing through chromatographic columns filled with the material to be characterized. Under the proper conditions, the partition of the solutes between the stationary and mobile phases is governed by steric (entropic) factors only. In this case it is possible to extract valuable information on the nanoporosity of the swollen polymer mass (gel) by mathematical treatment of the chromatographic data.

According to the Ogston model [23] the polymer chains in the gel are represented as randomly distributed, infinite-length cylindrical rods. The void space among them is filled by the swelling liquid and represents the nanopore system of the swollen polymer mass. The sum of chain lengths in a definite volume element over its volume (the polymer chain density, PCD, usually expressed as nm^{-2}) is the characteristic geometric parameter. From a qualitative point of view, it corresponds to the pore diameter in a conventional cylindrical pore description of porous materials. For the purpose of ISEC analysis, the swollen polymer mass is modeled as a set of discrete fractions, each characterized by a single value of PCD. Typical PCD values range from 0.1 nm^{-2}, corresponding roughly to the density of a solution of a linear polymer, up to 2 nm^{-2}, featuring very dense polymer regions into which even the smallest molecules can hardly penetrate. ISEC analysis yields the volume (V_i) of each fraction, usually referred to the unit mass of dry material. The sum of these values ($\sum V_i$) should be ideally equal to the total volume of the swollen polymer (gel volume, V_g). The latter can be determined experimentally from chromatographic data as the difference between the column volume and the elution volume of an eluate, which is totally excluded from the stationary phase. It should be appreciated that V_g values do not depend on modeling and are truly experimental. ISEC results on some investigated resins are collected in Table 7 for water-swollen materials. No data could be collected for ethanol because the condition of the sterically driven partition between the stationary and mobile phases is not met in alcohols [19].

In general, the fraction at PCD = 2.0 nm^{-2} is by far the most abundant. This means that most materials are not particularly accessible when swollen in water. This implies that a part of the polymeric mass is not involved in the partitioning of the eluates, that is, even the smallest of them cannot penetrate the whole volume of the swollen resin. However, as V_g is an experimental quantity, the relevant values can be compared safely. The data in Table 7 are consistent with those of Table 6 (BEV) in that they also demonstrates that the introduction of DMAA in CEA- and MA-based resins makes the materials more compatible with water in comparison with the homopolymers.

Table 7
PCD, $\sum V_i$, and V_g values for some resins swollen in water together (see the text for the meaning of the quantities)

Resin	Gel fraction volumes (V_i) ($cm^3\,g^{-1}$)							$\sum V_i$	V_g
D	PC	0.1	0.2	0.4	0.8	1.5	2.0	($cm^3\,g^{-1}$)	($cm^3\,g^{-1}$)
CF1		0.00	0.04	0.00	0.53	0.93	1.40	2.90	3.01
CF2		0.00	0.00	0.00	0.00	0.00	0.41	0.41	0.88
CF2-50		0.00	0.05	0.03	0.00	0.00	1.17	1.26	2.12
CF3		0.03	0.00	0.00	0.00	0.00	1.36	1.39	0.66
CF3{30}		0.00	0.00	0.00	0.00	0.00	0.74	0.74	0.65
CF3{50}		0.00	0.05	0.03	0.00	0.00	1.17	1.25	2.15
CF3{70}		0.00	0.10	1.01	0.00	0.00	0.83	1.94	2.64

Courtesy of Dr. Jerabek, Academy of Sciences of the Czech Republic, Prague.

3.5. Preparation of the catalysts: platination of the functional resins

The dispersion of Pt^0 inside of the functional resins was carried out along two main routes. The first is based on the impregnation of the resin with mesitylene solutions of colloidal platinum ("solvated metal atom") obtained with metal vapor synthesis techniques [15], hereafter referred to as MVS. The second procedure, hereafter referred to as CIR (chemical incorporation and reduction), implies the immobilization of convenient molecular platinum precursors in the pre-swollen resins, followed by chemical reduction of the metal center. In the case of the MVS route, metal nanoparticles are expected to reside in a resin outer layer, in view of the poor swelling of the support in mesitylene.

The choice of mesitylene as the liquid medium for the deposition of the solvated metal atoms could seem awkward. Ethanol, which is able to swell the supports and is employed as a solvent in the catalytic runs, seems to be a better alternative in this respect. However, mesitylene is the more convenient ligand for stabilizing Pt atoms obtained via MVS. The co-condensation of Pt-vapor and mesitylene affords products that are soluble in the excess of mesitylene, stable at relatively low temperature (−30 °C), and very suitable for gently reacting with supports depositing active Pt(0) particles under very mild conditions [24]. Protic solvents, such as ethanol, can react with vapors of transition metal elements affording in situ catalytic species such as metal hydrides, as evidenced, for example, in the case of Ni vapors [25].

In the case of CIR, the distribution of the platinum nanoclusters throughout the resin particles is expected to be essentially homogeneous [17], provided that both the metal precursor immobilization and its subsequent reduction are carried out under conditions of full swelling of the polymeric supports. Unfortunately, this is unfulfilled with almost all of them; hence very poorly active CIR catalysts are generally obtained. Only with CF3{70}, which has a fair capacity for swelling in the required solvents, it is possible to obtain a CIR catalyst, which is even more effective than the best MVS. The catalysts obtained are listed in Table 8, along with their metal content.

Table 8
Platinum contents of CIR and MVS catalysts

Catalyst	(%) Pt (w/w)
CIR-CF3{70}/Pt	0.59
MVS-CF1/Pt	0.9%
MVS-CF2/Pt	1.0%
MVS-CF3/Pt	0.8%
MVS-CF4/Pt	1.0%

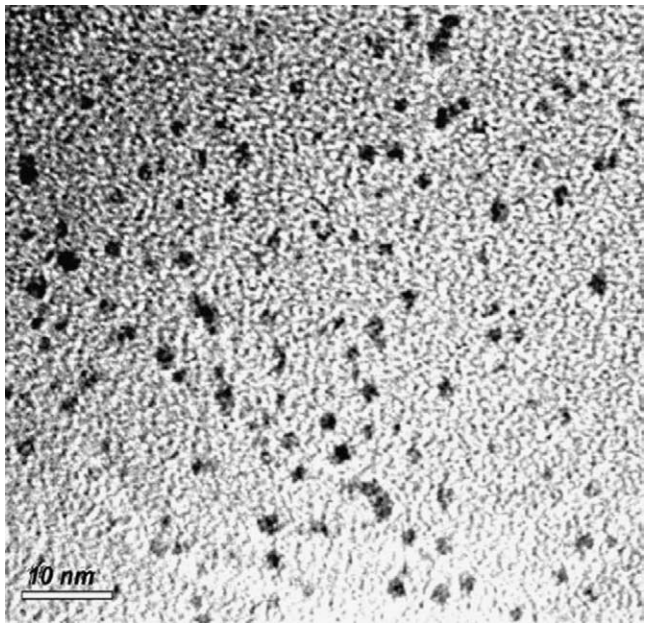

Fig. 3. TEM picture of MVS-CF1/Pt ($10^5\times$).

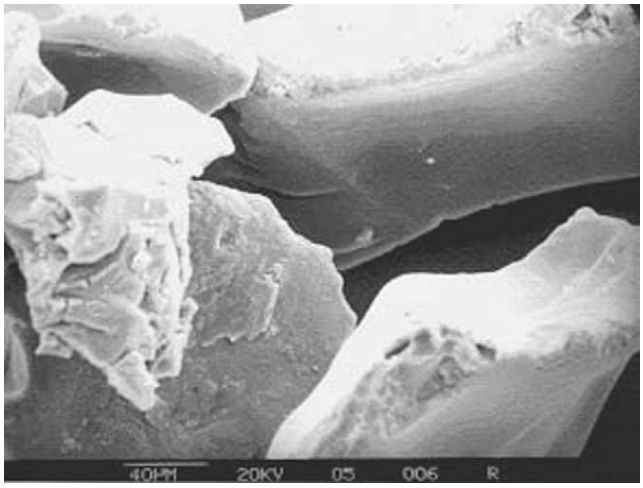

Fig. 4. SEM picture of MVS-CF2/Pt (500×).

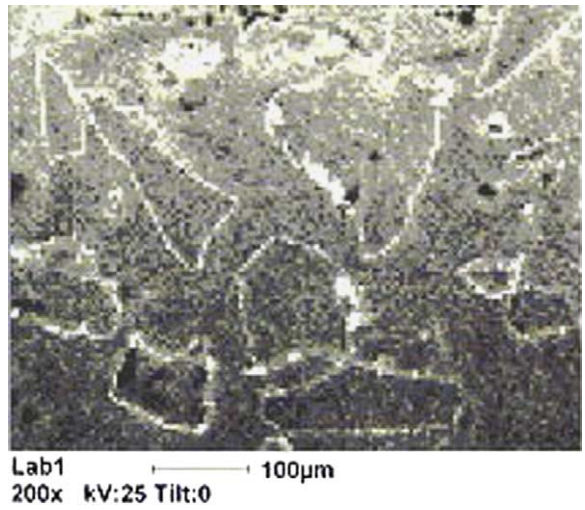

(a)

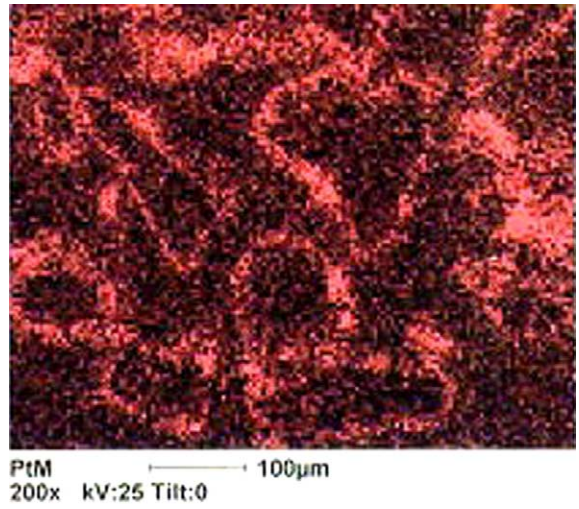

(b)

Fig. 5. SEM picture (a) and Pt XRMA analysis (b) of MVS-CF2/Pt (200×).

MVS-CF1/Pt is a black powder consisting of irregularly shaped microparticles. TEM microphotographs (Fig. 3) show the presence of spherical metal nanoclusters with diameters around 2 nm.

MVS-CF2/Pt is a black powder consisting of 100–180-µm, irregularly shaped microparticles. SEM microphotographs (Fig. 4) show the expected glassy aspect, with some macroscopic, structurally irrelevant fractures.

XRMA analysis of MVS-CF2/Pt (Fig. 5) shows that the metal nanoclusters lie in a peripheral layer roughly 10 µm thick. This observation agrees with the negligible swelling of the resin in mesitylene.

TEM analysis of ultrathin sections (ca. 400 nm thick) of MVS-CF2/Pt particles reveals that even in the outer shell the platinum nanoparticles are not homogeneously distributed. In fact, they form 50–200-nm thick sublayers, likely corresponding to the surface of the accessible polymer domains (Fig. 6). TEM microphotographs at higher magnification of ultrafinely ground particles of the *as prepared* catalyst, showed that platinum nanoclusters are roughly spherical in shape, with diameters of 2–3 nm.

MVS-CF3/Pt looks very much like MVS-CF2/Pt, and their SEM microphotographs are very similar (Fig. 7).

XRMA analysis (Fig. 8) reveals, as expected, the same metal distribution of the platinum nanoclusters in the polymeric particles as in MVS-CF2, with a metal-containing layer a few micrometers thick.

TEM characterization yields results similar to those for MVS-CF2/Pt (Fig. 9).

MVS-CF4/Pt is also a black powder. TEM analysis of ultrathin sections and of the powder as such (Fig. 10) yields a picture similar to those of MVS-CF2/Pt and MVS-CF3/Pt.

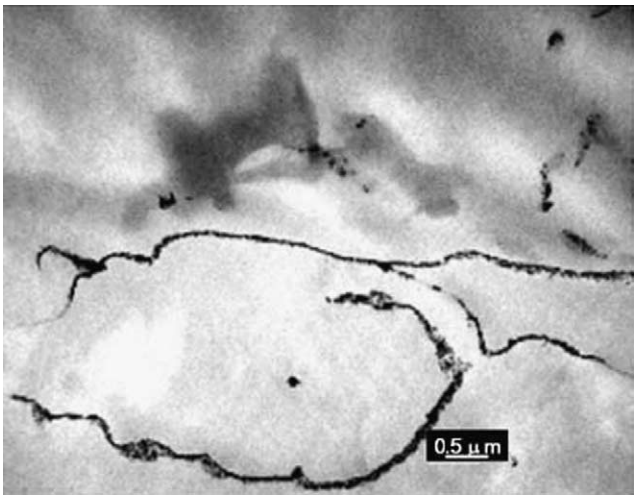

(a)

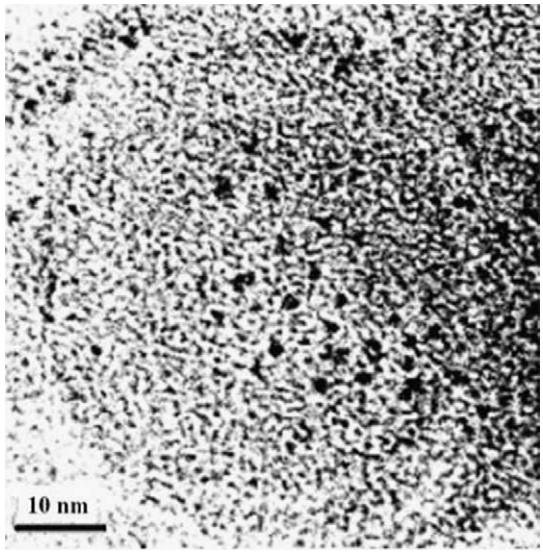

(b)

Fig. 6. TEM picture of an ultrathin section of a MVS-CF2/Pt particle (a) and TEM picture of Pt^0 nanoclusters in MVS-CF2/Pt (b).

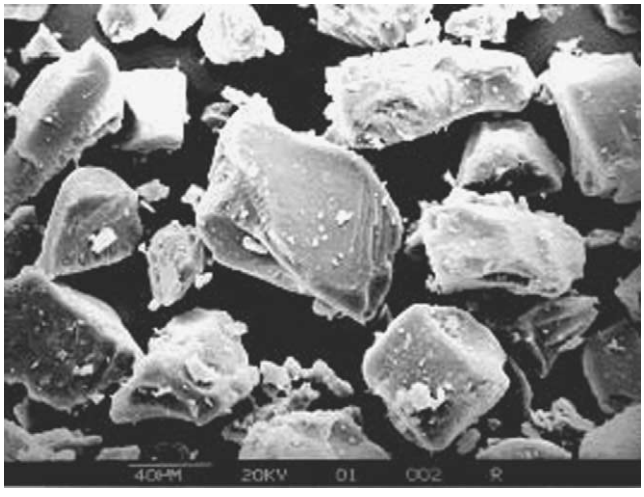

Fig. 7. SEM picture of MVS-CF3/Pt (500×).

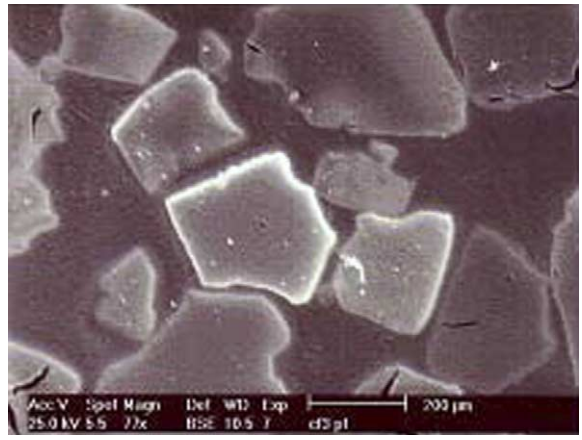

(a)

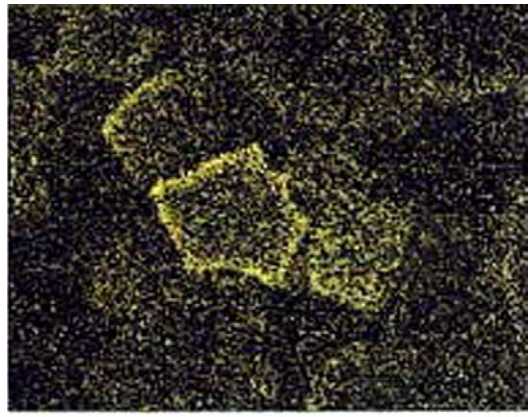

(b)

Fig. 8. SEM picture (a) and Pt XRMA analysis (b) of MVS-CF3/Pt.

The metal lies in thin layers, a few tens of nanometers thick, stretching out across the catalyst particles. Platinum nanoclusters are spherically shaped, with diameters around 2–3 nm. Therefore, no appreciable differences in the distribution or in the metal nanocluster sizes are observed from one MVS catalyst to the other. These features are apparently independent of the nature of the support and seem to be dictated simply by the preparation method.

CIR-CF3{70}/Pt is a dark brown powder consisting of irregularly shaped granules. The catalyst is obtained upon exchanging fixed Na^+ ions of the resin with $[Pt(NH_3)_4]^{2+}$ cations. This operation is carried out in water, where CF3{70}/Na swells very well and the metal complex is soluble. Platinum is then reduced with an alcoholic solution of $NaBH_4$. XRMA analysis shows that its radial distribution throughout the catalyst beads is fairly homogeneous (Fig. 11). TEM microphotographs show irregularly shaped nanoclusters, a few tens of nanometers across (Fig. 11). Relatively large nanoclusters are actually aggregates of small, worm-like nanoparticles, about 2 nm thick and up to about 5 nm long (Fig. 11).

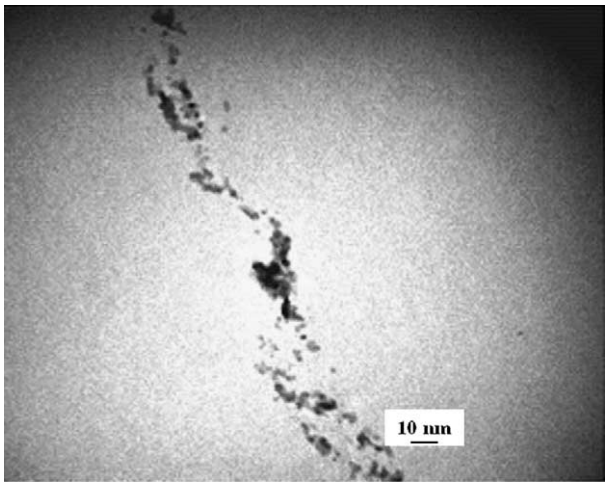

(a)

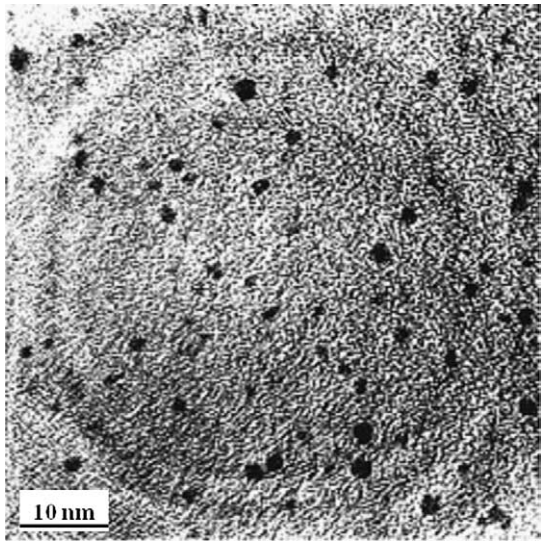

(b)

Fig. 9. TEM picture of an ultrathin section of a MVS-CF3/Pt particle (a) and TEM picture of Pt^0 nanoclusters in MVS-CF3/Pt (b).

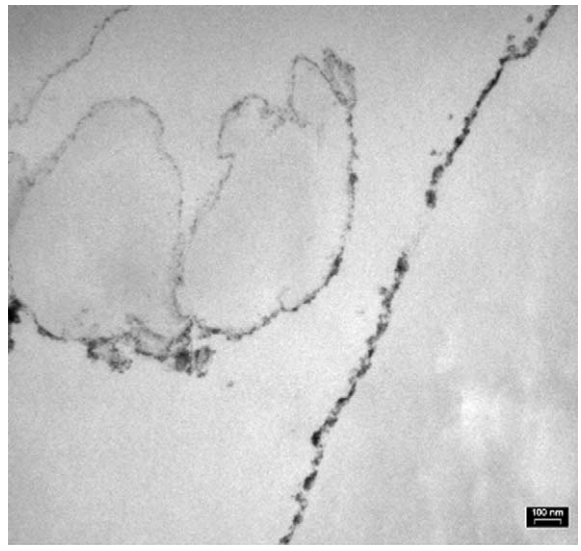

(a)

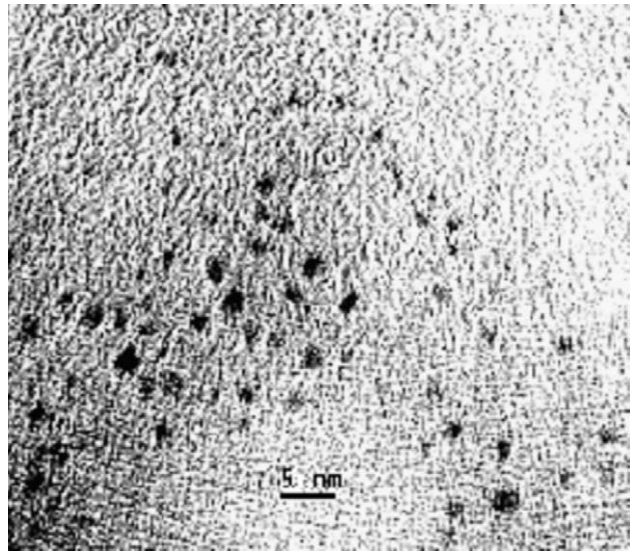

(b)

Fig. 10. TEM picture of an ultrathin section of a MVS-CF4/Pt particle (a) and TEM picture of Pt^0 nanoclusters in MVS-CF4/Pt (b).

3.6. Preparation of the catalysts: platination of the Lewis-acid-modified resins

In line with the premises of this work (Fig. 1), some MVS catalysts (Table 9) were prepared by platination of CF3 and CF4 modified with metal ions (Lewis acids).

The resins were metalated with Fe^{II}, Co^{II}, and Zn^{II} acetates prior to platinum deposition. CF4 was metalated with a solution of cobalt(II) acetate in ethanol. BEV data show that upon conversion of the carboxylic groups of CF3 into carboxylate groups, the degree of swelling of the resin drops dramatically in ethanol and increases remarkably in water. As a consequence, the progressive replacement of H^+ ions of –COOH groups in CF3 with divalent metal ions was expected to cause a drastic decrease in the degree of swelling during the ion-exchange process, making it more and more difficult. Thus water solutions of the acetates were used for the metalation of CF3. The presence of Lewis acids is expected to enhance the selectivity for the desired unsaturated alcohols [1]. The reaction between the metal ions and the resin (ion exchange for CF3, metal coordination to pyridyl rings for CF4) is generally facile. Extensive incorporation of the metal centers is generally observed. XRMA reveals a nicely homogeneous distribution of the metal centers in

Table 9
Metal contents in MVS-CF*n*/M/Pt ($n = 3, 4$; M = Fe, Co, Zn) catalysts

Catalyst	(%) Pt (w/w)	(%) M (w/w)	M/Pt (mol/mol)
MVS-CF3/Fe/Pt	0.71	8.2	40
MVS-CF3/Co/Pt	0.89	14.1	52
MVS-CF3/Zn/Pt	0.43	15.2	105
MVS-CF4/Co/Pt	2.5[a]	6.2	8

[a] Estimated from the complete fading of the solvated platinum atoms solution employed for the impregnation.

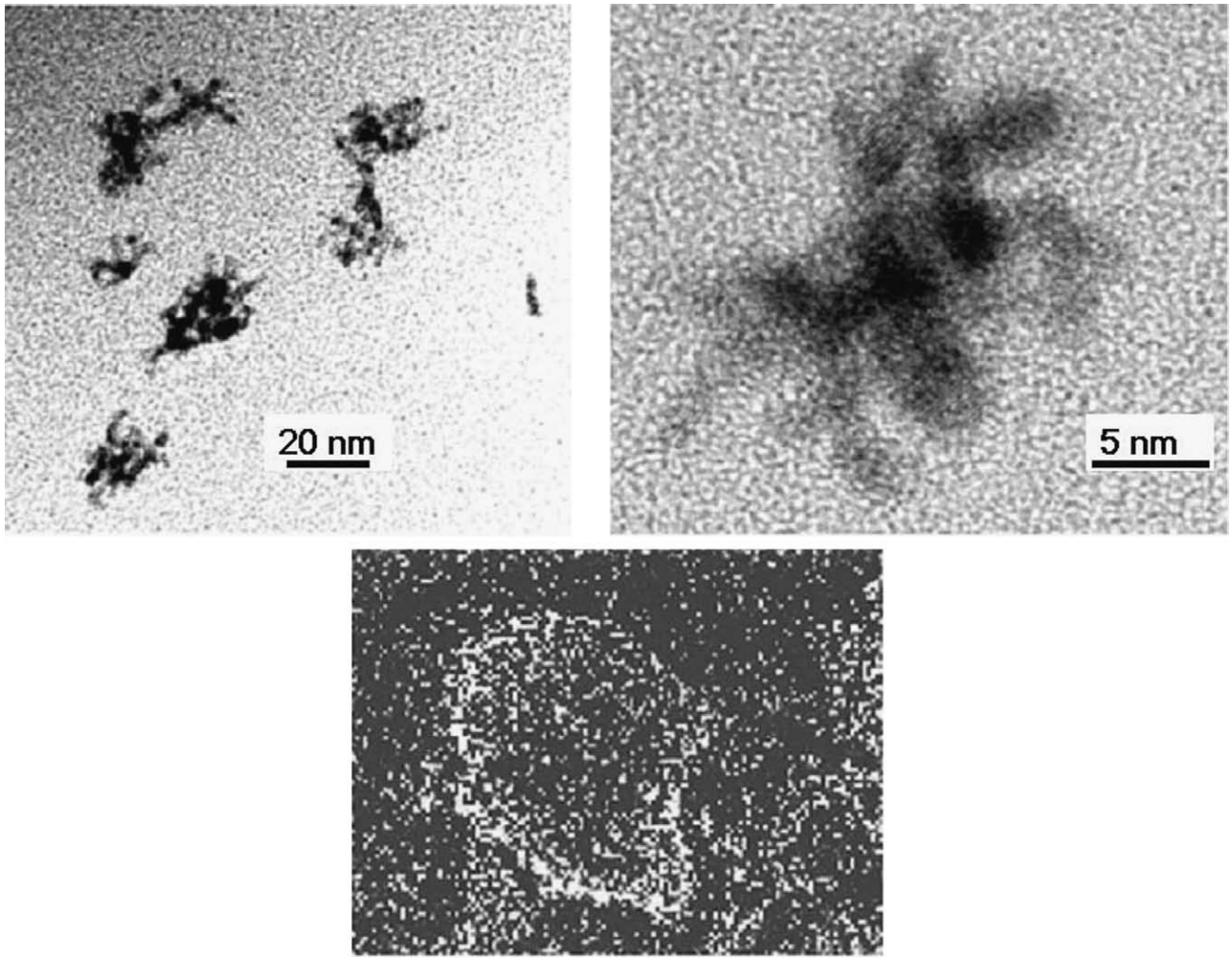

Fig. 11. TEM and XRMA pictures of CIR-CF3{70}/Pt.

CF3 for cobalt and zinc (Figs. 12 and 13). In the case of iron some accumulation of the promoter toward the particle edges is observed (Fig. 14).

Samples of resins modified with different Lewis acids are treated with solutions in mesitylene of solvated platinum atoms, to give the final promoted MVS catalysts. MVS-CF3/Co^{II}/Pt exhibits an intense violet color and is characterized by TEM. Pt^0 nanoclusters appear to be fairly regular in size (2–4 nm) (Fig. 15).

XRMA analysis for platinum was not carried out in the promoted MVS catalysts. Its radial distribution is supposed to be in the shape of an egg-shell, just like in the other MVS catalysts investigated in this work.

3.7. Catalytic results

Under the experimental conditions described here, the hydrogenation of citral (3,7-dimethyl-2,6-octadienal) over Pt-supported catalysts occurs through a reaction pathway that is summarized in Scheme 1. Geraniol (*trans*-3,7-dimethyl-2,6-octadienol) and nerol (*cis*-3,7-dimethyl-2,6-octadienol) are formed by hydrogenation of the C=O group of the (E) and (Z) isomers of citral, respectively. Citronellal (3,7-dimethyl-6-octenal) is obtained by the parallel hydrogenation of the conjugated C=C double bond. Citronellol (3,7-dimethyl-6-octen-1-ol) is formed by hydrogenation of citronellal and/or geraniol and nerol. Isopulegol (2-isopropyl-5-methyl-cyclohexanol), a cyclization product of citronellal, and the diethylacetal of citronellal were never observed. The catalytic results are illustrated in Fig. 16. Activities are assessed as the initial reaction rate per unit mass of platinum (mol g_{Pt}^{-1} s^{-1}).

The most intriguing information conveyed in Fig. 16 is the remarkable selectivity of the MVS catalysts supported by CF2, CF3, and CF4. The last is not particularly active, and the reaction stopped at low conversion ($\leqslant$ 20–30%) with 54% selectivity. For MVS-CF2/Pt and MVS-CF3/Pt the hydrogenation proceeds to high conversion ($\geqslant$ 80–90%), with no appreciable difference in the selectivity for the unsaturated alcohols (46–47%) at low and high conversion. It could be argued that the hydrogenation of the C=C bond is more favored than the hydrogenation of the conjugated C=O bond at 70 °C (the reaction temperature used in the present work). In fact it is well known that the former is favored over the

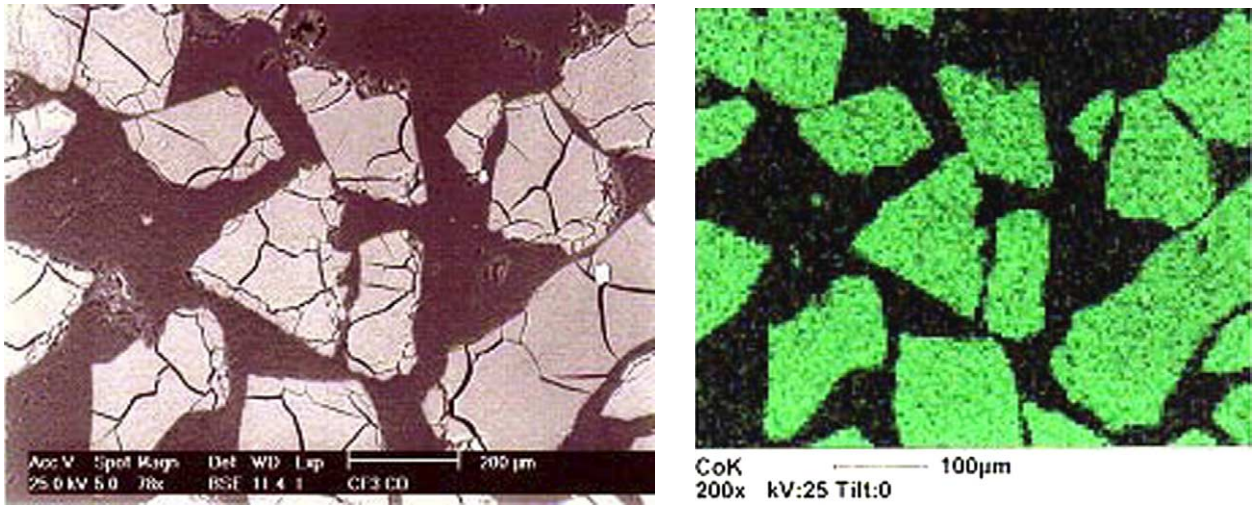

(a) (b)

Fig. 12. SEM (a) and XRMA (b) analysis of a section of CF3/Co^{II}. Cobalt distribution is seen to be homogeneous.

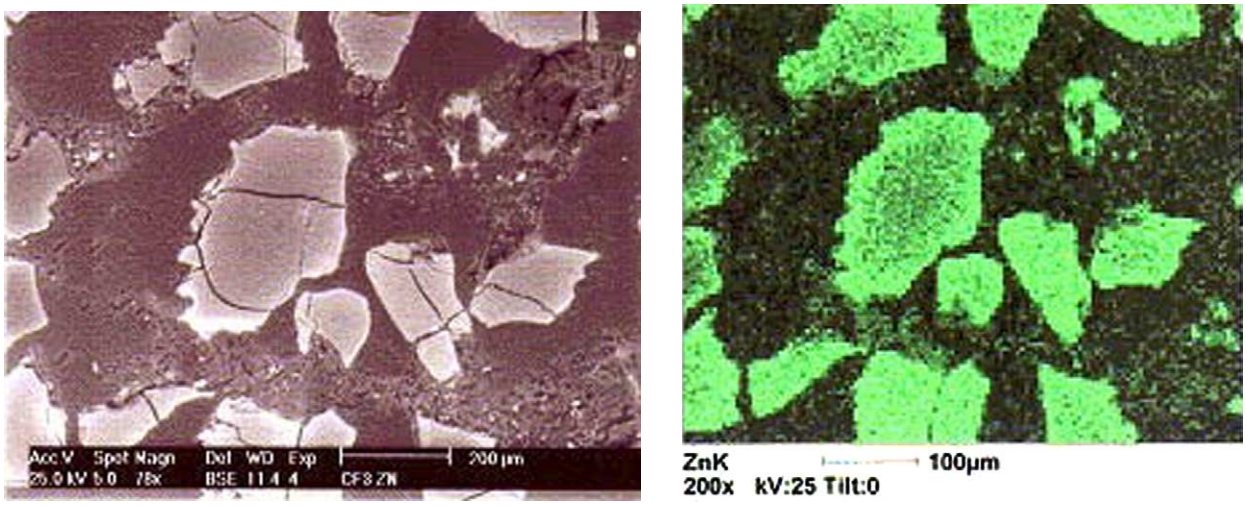

(a) (b)

Fig. 13. SEM (a) and XRMA (b) analysis of a section of CF3/Zn^{II}. Zinc distribution is homogeneous.

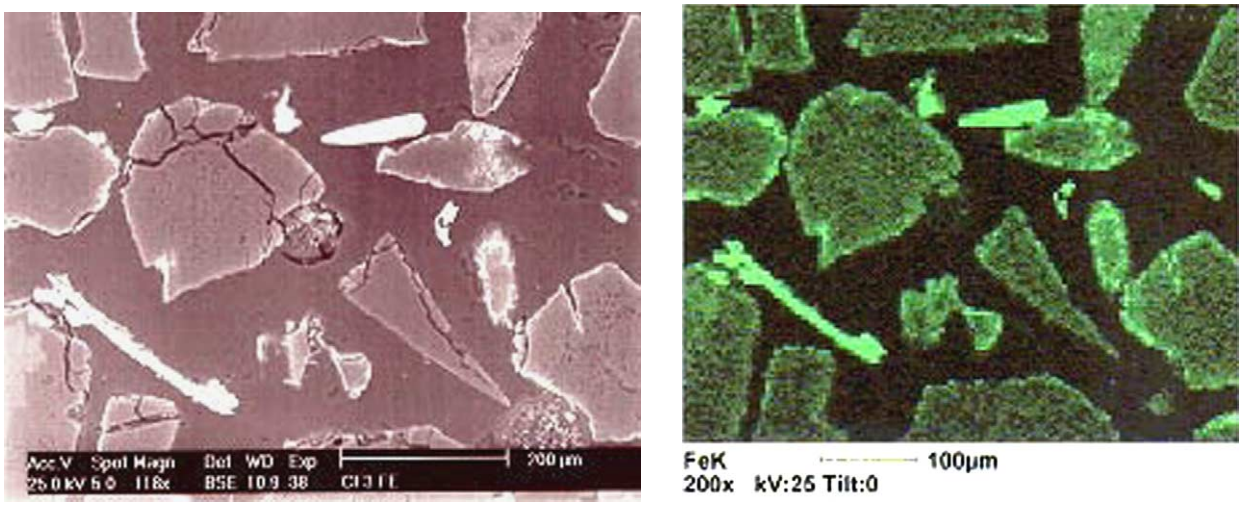

(a) (b)

Fig. 14. SEM (a) and XRMA (b) analysis of a section of CF3/Fe^{II}. A modest accumulation of the element at the particles edges is apparent.

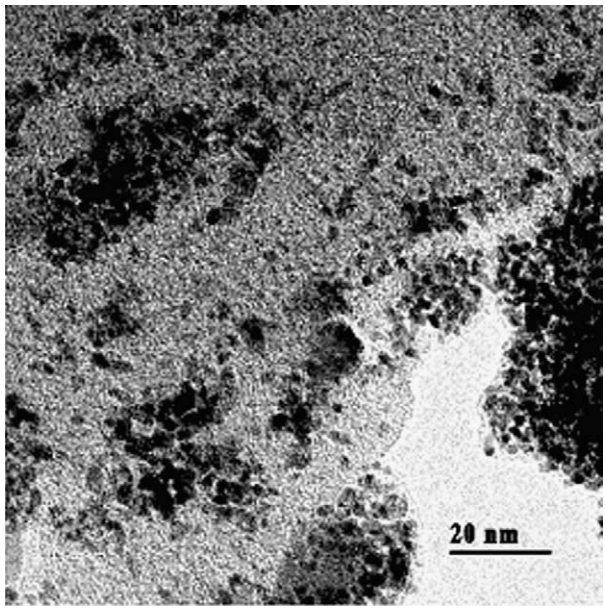

(a)

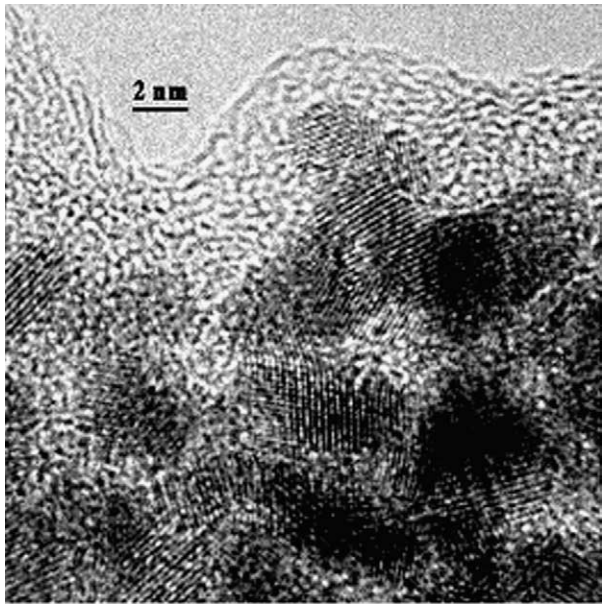

(b)

Fig. 15. TEM picture of MVS-CF3/Co^{II}/Pt: low resolution (a); high resolution (b).

latter at low temperature and that the selectivity towards unsaturated alcohols can be enhanced by increasing the reaction temperature [26]. However, we have found that in the hydrogenation of citral on monometallic catalysts under conditions otherwise identical to those applied in the present work, Pt catalysts supported on SiO_2 and Al_2O_3 show a selectivity for the formation of unsaturated alcohols lower than 20%. This rules out the reaction temperature as the possible cause of the unexpectedly high selectivity observed.

As shown above, all of the MVS catalysts, including the poorly selective MVS-CF1/Pt, exhibit similar a nanocluster size (2–3 nm) and size distribution. Therefore the degree of

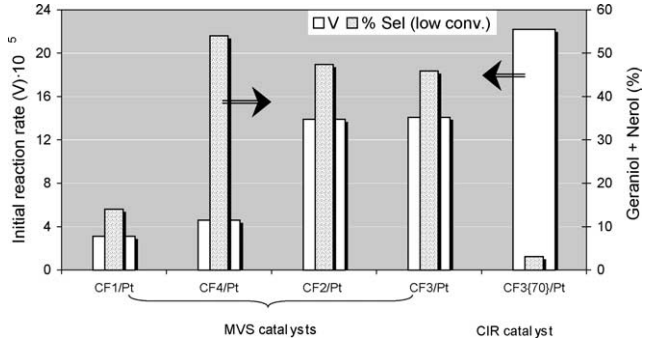

Fig. 16. Observed initial reaction rates (mol g_{Pt}^{-1} s^{-1}) and selectivity to geraniol/nerol at low (20–30%) conversion of citral for the monometallic MVS catalysts; for MVS-CF2/Pt and MVS-CF3/Pt selectivity at high conversion (80–90%) are unchanged.

metal dispersion does not seem to affect the selectivity for these platinum catalysts; that is, the reaction is structure insensitive.

The presence of a second metallic species can enhance the selectivity for unsaturated alcohols [1]. This was the case, for instance, for Ru/C catalysts, which exhibited a 35% selectivity for geraniol/nerol in the hydrogenation of citral due to the presence of impurities (mainly Fe) on the surface of the carbon support [27]. Therefore, care must be taken to avoid the unintended introduction (contamination) of even trace amounts of potential metal promoters during the catalyst's preparation. Accidental catalyst's contamination (and undesired promotion) does not seem to pertain to the MVS catalysts described here, in that they are not invariably selective. MVS-CF1/Pt, for instance, shows a low selectivity, comparable to that of unpromoted Ru/Al_2O_3 catalysts under similar experimental conditions [28].

In conclusion, the selectivity seems to depend on the nature of the polymeric support, which possesses functional groups that could interact with the platinum nanoclusters. CF2 and CF4 feature electron-donating functions (cyano and pyridyl, respectively). It is well known that basic substances added to the reaction mixture are strongly able to increase the selectivity towards unsaturated alcohols in the hydrogenation of α,β-unsaturated aldehydes [1]. This strongly suggests a direct interaction of the basic cyano and pyridyl groups with the metal nanocluster surface, which makes the metal catalyst fairly selective. On the other hand, CF3 does not contain a basic function, but the effect of oxygenated groups has already been invoked for platinum catalysts supported by surface-oxidized activated carbon [29]. In addition, acetic acid itself has been reported to be an effective promoter in the hydrogenation of 2-methyl-2-pentenal over Co-Raney in the liquid phase [30].

The only useful CIR catalyst obtained is CIR-CF3{70}/Pt, which is the most active among those described in this paper. The initial reaction rate over this catalyst (ca. 23 mol g_{Pt}^{-1} s^{-1}) is almost double with respect to the most active MVS catalysts, and the reaction proceeds up to high conversion of the substrate. However, this CIR catalyst is

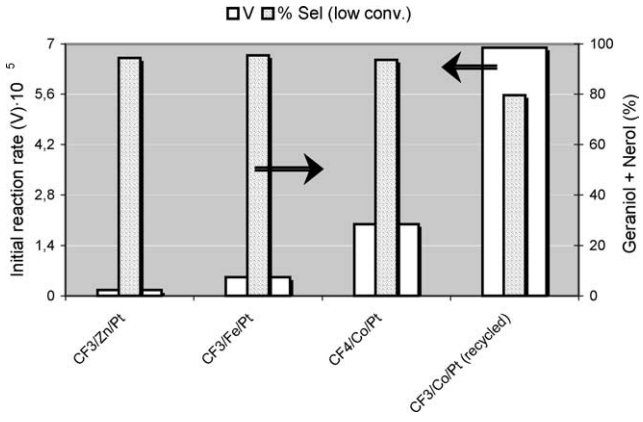

Fig. 17. Observed initial reaction rates (mol g_{Pt}^{-1} s^{-1}) and selectivity to geraniol/nerol at low (20–30%) conversion of citral for MVS bimetallic catalysts; for MVS-CF4/Co/Pt and MVS-CF3/Co/Pt the selectivity at high conversion (80–90%) are unchanged.

very poorly selective, in contrast, for instance, with MVS-CF3/Pt, which also possesses carboxylic groups. As the selectivity enhancement in monometallic MVS catalysts can be attributed to the interaction of the metal with the functional groups of the support, this observation indicates that the functional groups of CF3{70} are not able to promote the platinum selectivity in the CIR catalyst. In this case the metal nanoparticles are much larger and irregularly shaped in comparison with MVS catalysts, and we argue that the interaction, if any, of the metal nanoparticles with the functional groups of the polymeric supports is not effective.

It is well known that the selectivity of the hydrogenation of α,β-unsaturated aldehydes over heterogeneous metal catalysts can be dramatically improved by a number of soluble promoters (see, for example, Refs. [31,32]), including several metal halides [33]. As shown above, the polymeric supports used in this work allow easy immobilization of a number of metal ions, through either ion-exchange or metal coordination. The resins (CF3 and CF4) modified with Fe(II), Co(II), or Zn(II) metal ions can be used as supports for platinum catalysts; the relevant catalytic data are illustrated in Fig. 17.

With Zn(II) and Fe(II) the selectivity for the formation of unsaturated alcohol is higher than 90%, but in comparison with the parent monometallic catalyst, their activity is severely hampered (1–3% of the activity of MVS-CF3/Pt). Better results are obtained with cobalt(II). The reaction over MVS-CF3/Co/Pt and MVS-CF4/Co/Pt proceeds up to high conversion of the substrate ($\geqslant$ 80–90%) with both catalysts. A remarkable enhancement of the selectivity, practically independent of the conversion, for geraniol/nerol has also been obtained, with a relatively small decrease (50%) in activity in comparison with the unpromoted parent catalysts.

To summarize, the catalysts promoted with Lewis acids (the immobilized metal ions) are much more selective, but less active, than the corresponding unpromoted ones. A similar effect was reported when soluble Lewis acids (halides of transition and nontransition elements) were added in large amounts to the reaction mixtures in the liquid-phase hydrogenation of α,β-unsaturated aldehydes over heterogeneous Pt/nylon catalysts [33]. In that case, the selectivity enhancement and the deactivation were attributed to the electrophilic C=O activation [1] and catalyst poisoning (site blocking), respectively.

In our catalysts the promoters are present in such a large amount in comparison with platinum (see Table 9) that site blocking can be envisaged, in spite of the different spatial distribution of the metal ions and platinum nanoclusters throughout the catalyst beads. However, site blocking implies the direct interaction of the poison (the promoter in large amounts) with the platinum surface. This requires that the poison is close enough or can readily come close to the metal surface. Some of us recently found that the size of polymer-supported metal nanoclusters is strictly comparable to that of the "pores" of the support [34]. This broadly implies that the functional groups of the polymer chains are at short distance from the metal surface in materials of this kind. In our catalysts the metal ions should lie very close to the platinum surface, as sketched in Fig. 1, and site blocking should therefore be possible.

4. Conclusions

Resin-supported platinum catalysts prove to be effective in the selective hydrogenation of an α,β-unsaturated aldehyde, citral, under mild conditions. In particular, the impregnation of the supports with solvated platinum atoms prepared with the MVS technique allows the generation of 2–3-nm, regularly shaped, spherical platinum nanoclusters. Monometallic Pt catalysts supported on CF2, CF3, or CF4 resins show a remarkably high selectivity for the formation of the unsaturated alcohols geraniol and nerol, as the result of the interaction of the metal with the groups of the functional polymeric supports. The addition of ions such as Fe(II), Co(II), and Zn(II) to the polymer framework of the support is easy. The introduction of ions of a second metal into the polymer framework of the support generally enhances the selectivity for geraniol/nerol, but deactivates the catalysts. This finding could be due to site blocking on the platinum surface with the second metal, which lowers the number of active sites available for the reaction.

Acknowledgments

This work was partially supported by PRIN Funding, 2001–2003, Ministero dell'Università e della Ricerca Scientifica, Italy (Project 2001038991). We are indebted to Dr. Karel Jerabek for ISEC measurements. Dr. Maria Gianmatteo is also gratefully acknowledged for TEM characterization. We are grateful to Dr. Riccardo Gallina for the synthesis of catalysts based on CF4.

References

[1] P. Gallezot, D. Richard, Catal. Rev.-Sci. Eng. 40 (1998) 81–126.
[2] W. Yu, Y. Wang, H. Liu, J. Mol. Catal. A: Chem. 112 (1996) 105.
[3] For a recent reference see M. Abid, F. Ammari, W. Zheng, K. Liberkova, R. Tourude, Stud. Surf. Sci. Catal. 145 (2003) 267–270, and references therein.
[4] For a recent reference see P. Reyes, H. Rojas, G. Pecchi, J.L.G. Fierro, J. Mol. Catal. A: Chem. 179 (2002) 293–299, and references therein.
[5] U.K. Singh, M.A. Vannice, J. Catal. 199 (2001) 73–84.
[6] R. Malathi, R.P. Viwanath, Appl. Catal. A: Gen. 208 (2001) 323–327.
[7] (a) S.R. de Miguel, M.C. Roman-Martinez, D. Cazorla-Amoros, E.L. Jablonski, O.A. Scelza, Catal. Today 66 (2001) 289–295;
(b) G. Lafaye, T. Ekou, C. Micheaud-Especel, C. Montassier, P. Marecot, Appl. Catal. A: Gen. 257 (2004) 107;
(c) F. Delbecq, P. Sautet, J. Catal. 220 (2003) 115.
[8] X. Chen, H. Li, W. Dai, J. Wang, Y. Ran, M. Qiao, Appl. Catal. A: Gen. 253 (2003) 349.
[9] See, for example, P. Reyes, H. Rojas, J.L.G. Fierro, Appl. Catal. A: Gen. 248 (2003) 59–65.
[10] See, for example, A.B. da Silva, E. Jordao, M.J. Mendes, P. Foilloux, Appl. Catal. A: Gen. 148 (1997) 253–264.
[11] See, for example, G.F. Sartori, M.L. Casella, G.J. Siri, H.R. Aduriz, O.A. Ferrelti, Appl. Catal. A: Gen. 197 (2000) 141–149.
[12] W. Yu, H. Liu, X. An, J. Mol. Catal. A: Chem. 129 (1998) L9–L13.
[13] K. Ramberg, Z. Anorg. Chem. 83 (1913) 35.
[14] M. Kralik, V. Kratky, M. De Rosso, M. Tonelli, S. Lora, B. Corain, Chem. Eur. J. 9 (2003) 209.
[15] G. Vitulli, M. Bernini, S. Bertozzi, E. Pitzalis, P. Salvadori, S. Coluccia, G. Martra, Chem. Mater. 14 (2002) 1183, and references therein.
[16] A.A. D'Archivio, L. Tauro, L. Galantini, A. Panatta, E. Tettamanti, M. Gianmatteo, K. Jerabek, B. Corain, submitted for publication.
[17] B. Corain, P. Centomo, S. Lora, M. Kralik, J. Mol. Catal. A: Chem. 204–205 (2003) 755–762, and references therein.
[18] R. Arshady, Adv. Mater. 3 (1991) 182.
[19] (a) K. Jerabek, Anal. Chem. 57 (1985) 1598;
(b) K. Jerabek, in: M. Potschka, P.L. Bubbin (Eds.), Cross Evaluation of Strategies in Size Exclusion Chromatography, in: ACS Symposium Series, vol. 635, American Chemical Society, Washington, DC, 1996, p. 211.
[20] B. Corain, M. Zecca, K. Jerabek, J. Mol. Catal. A: Chem. 177 (2001) 3.
[21] K.W. Pepper, D. Reichenberg, D.K. Hale, J. Chem. Soc. (1952) 3129.
[22] B. Corain, M. Zecca, K. Jerabek, J. Mol. Catal. A: Chem. 177 (2001) 3.
[23] A.G. Ogston, Trans. Faraday Soc. 54 (1958) 1754.
[24] G. Vitulli, R. Falorni, P. Salvadori, Catal. Lett. 17 (1993) 151–155.
[25] S. Bertozzi, C. Iannello, G. Barretta Uccello, G. Vitulli, R. Lazzaroni, P. Salvadori, J. Mol. Catal. 77 (1992) 1–6.
[26] (a) U.K. Singh, A. Vannice, J. Catal. 191 (2000) 165–180;
(b) U.K. Singh, M.N. Sysak, A. Vannice, J. Catal. 191 (2000) 181–191.
[27] S. Galvagno, C. Milone, A. Donato, G. Neri, Catal. Lett. 18 (1993) 83.
[28] L. Mercadante, G. Neri, C. Milone, A. Donato, S. Galvagno, J. Mol. Catal. A: Chem. 105 (1996) 93.
[29] F. Coloma, A. Sepúlveda-Escribano, F. Rodríguez-Reinoso, Appl. Catal. A 123 (1995) L1.
[30] K. Hotta, T. Kubomatsu, Bull. Chem. Soc. Jpn. 46 (1973) 3566.
[31] G. Neri, C. Milone, A. Donato, L. Mercadante, A.M. Visco, J. Chem. Tech. Biotech. 60 (1994) 83.
[32] G. Neri, L. Mercadante, C. Milone, R. Pietropaolo, S. Galvagno, J. Mol. Catal. A: Chem. 108 (1996) 41.
[33] S. Galvagno, A. Donato, G. Neri, R. Pietropaolo, D. Pietropaolo, J. Mol. Catal. A: Chem. 49 (1989) 223.
[34] B. Corain, K. Jerabek, P. Centomo, P. Canton, Angew. Chem., Int. Ed. 43 (2004) 959–962.